Key Engineering Materials
ISSN: 1662-9795, Vol. 1050, pp 21-30
doi:10.4028/p-5MlW2P
© 2026 The Author(s). Published by Trans Tech Publications Ltd, Switzerland.
Submitted: 2026-01-05
Revised: 2026-02-18
Accepted: 2026-02-18
Online: 2026-04-16

Multi-Objective Bayesian Optimization of Dual-Phase Steel Microstructures for Minimal Damage Initiation

Irene Biermann[1,a*], Niklas C. Fehlemann[1,b], Maximilian Hribsek[1,c] and Sebastian Münstermann[1,d]

[1]Institute of Metal Forming, RWTH Aachen University, Intzestraße 10, 52072 Aachen, Germany

[a]irene.biermann@ibf.rwth-aachen.de, [b]niklas.fehlemann@ibf.rwth-aachen.de, [c]maximilian.hribsek@ibf.rwth-aachen.de, [d]Sebastian.Muenstermann@iehk.rwth-aachen.de

Keywords: Dual-Phase Steel, Microstructure Optimization, Bayesian Optimization

Abstract. Gaining a better understanding of the structure-property relationship in materials is a vital step in optimizing forming processes in order to minimize the induced damage and thereby maximizing the materials' performance. Dual phase (DP) steels are comprised out of hard martensite surrounded by a soft and ductile ferrite matrix. Due to the complex microstructure of DP-steels, different mechanisms of damage initiation can occur, such as martensite cracking or ferrite-martensite phase boundary decohesion. A key problem with computational microstructure optimization focusing on one specific damage mechanism is, that this can lead to virtual microstructures, which are good against one mechanism, but vice-versa problematic for another mechanism. This is why all optimization strategies have to consider more than one mechanism. In this study, a multi-objective Bayesian optimization (moBo) approach is developed for the design of damage-tolerant DP-microstructures. It combines full-field crystal plasticity simulations on 3D representative volume elements with computational optimization. By employing the moBo, the sets of microstructure parameters are determined, where the combined minimum of both damage indicators is located. The proposed algorithm was applied to identify pareto-optimal microstructure configuration for DP800, considering both prevalent damage mechanisms It also provides an estimate of the variance associated with each parameter, which defines how critical the correct regulation of that aspect is. The results are in line with prevailing knowledge about DP steel, thus showing that the proposed approach is a promising tool for computational microstructure design

Introduction

Finding the optimal combination of microstructure parameters for minimal damage initiation during forming is an important step in creating reliable components. The mechanical properties of dual phase steel are highly dependent on their complex microstructure, not only the grain sizes but also the distribution of the phases or the hardness contrast between both phases have an impact [1]. Since the performance of a formed component is heavily influenced by the damage behavior of its microstructure [2], this study aims to optimize the microstructure parameters with respect to damage initiation during plastic deformation. The material this paper is based on is a DP800 steel containing ferrite and martensite. In the investigated material, two main damage mechanisms are observed: cleavage fracture of the martensite, and ferrite-martensite phase boundary decohesion [3]. If the optimization focuses on just one of the damage mechanisms, it could result in microstructures that perform poorly for the other one. Thus, a multi-objective optimization framework is used to find Pareto-optimal states for both damage mechanisms. For the task of optimizing computationally expensive black-box functions, Bayesian optimization is well suited [4].

In this study, multi-objective Bayesian optimization was used to find microstructure parameters of dual-phase steel that promise minimal damage initiation during plastic deformation. In combination with the Sobol indices of the parameters these findings can be used to create damage-resistant materials. In the final step, the validity of the results is assessed by comparing the findings with the existing literature.

This article is an open access article under the terms and conditions of the Creative Commons Attribution (CC BY) license (https://creativecommons.org/licenses/by/4.0)

The effects of microstructure features on the damage initation in dual phase steels have already been described in previous studies [3] and quantified by Fehlemann et al. [5]. However, this paper offers a novel approach for damage-resistant materials design by employing target-oriented multi-objective Bayesian optimization to find Pareto-optimal states.

Methods

This study was performed using DP800 steel, consisting of a ferrite matrix and martensite islands and banded structures. The base material contains around 30% martensite without retained austenite or bainite [5]. In uniaxial tension tests the material showed an ultimate elongation of 20% [5]. The heterogenous microstructures shows significant banding in some areas while in others only martensite islands are present. The base materials' crystal plasticity parameters were determined in a previous study by Fehlemann et al. [7] using in situ micropillar compression experiments [8].

All simulations are performed on statistical representative volume elements (sRVE) with an edge length of 32µm and a resolution of two. This size offers a good tradeoff between scatter and the time needed to generate the sRVE. To further reduce scatter, the band thickness is kept constant at 2.94µm, which is the median band thickness observed in the material [7]. The aim of this paper is to vary the microstructure of the base material to find the microstructure parameters that lead to minimal damage initiation during plastic deformation.

The varied parameters are:

- Phase ratio of ferrite and martensite (P_R)
- Grain sizes of ferrite and martensite (F_gr and M_gr)
- Aspect ratio of ferrite and martensite grains (F_ar and M_ar)
- Existence of martensite bands (N_b)
- Ferrite hardening (F_hard)

In the round brackets the abbreviations for the indicators used in the figures of this paper are given.

The parameters determining the grain sizes and morphology can be understood as resizing parameters. They modify the original values of the base material. This procedure is adapted from the work of Fehlemann et al. [5].

An overview of the optimization process is depicted in **Figure 1**. In the first step of the optimization, 50 microstructure parameter combinations are created that serve as initial data. The parameters are then used by the sRVE generator DRAGen to build the sRVE with the defined microstructure [9]. Afterwards, the open-source framework DAMASK is used to simulate the materials behavior under a uniaxial load [10]. In the last step, the amount of damage occurring in the sRVE is investigated, which is used as a basis for the acquisition function to choose the next points in the design space to investigate. Since the acquisition function is optimizing multiple metrics at once to find pareto-optimal states, an acquisition function for multi-objective optimization is used. In each epoch, the acquisition function chooses 20 parameter combinations for the next optimization step.

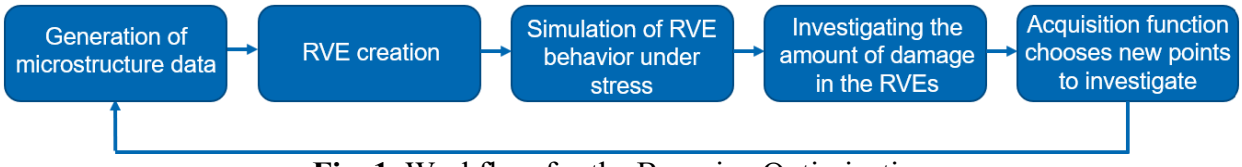

Fig. 1. Workflow for the Bayesian Optimization

In initial microstructure parameters are drawn from a Sobol sequence [11]. This promises optimal space filling of the design space. In the following epochs, the parameters are chosen by the acquisition function.

To create the sRVE, the microstructure data generated in the previous step gets passed to DRAGen. Since the sRVE generation process and the subsequent load simulation is quite noisy, two sRVE with equal microstructure parameters are generated.

Simulating the mechanical material behavior is done using the open-source, multi-physics framework DAMASK [10]. The procedure was already described extensively in [5] and will only be shortly outlined in this work. For the purpose of this paper, a simple uniaxial tension load case in rolling direction up to a strain of 12% was chosen. The strain rate was kept at 0.001. In future works, this could be expanded by simulating an actual load case that happens during metal forming. The simulations were done using a phenomenological crystal plasticity model [12] [13]. To model the martensite's mechanical behavior, an isotropic plasticity model available in DAMASK was utilized. This is applicable since the substructures of the martensite are not considered in the sRVE and the martensite's properties can therefore be considered to be isotropic. The experimental data is in line with this assumption [14]. The crystal plasticity model for this work was already calibrated and validated by Fehlemann et al. in [7] using *in situ* micropillar compression.

One of the varied parameters is the phase ratio of ferrite and martensite. Since the overall carbon content of the material is constant and almost all of the carbon is solved in the martensite, the carbon content in the martensite depends on the phase fraction. It has been observed in multiple studies, that the carbon content influences the martensite's hardness [15]. This effect was considered by using an approach proposed in [5]. In a first step, the Vickers hardness was calculated with respect to the carbon content using Toth's regression formula [16]. The Vickers hardness can then be used to estimate the tensile strength with the equation proposed by Pavlina and van Tyne [17]. For more detailed info on this procedure, the interested reader is referred to [5].

The main damage mechanisms in dual-phase steel are semi-brittle martensite cracking, martensite-ferrite phase boundary decohesion and ferrite fracture [3]. Since the latter is rarely observed in the steel investigated in this study, the two damage indicators applied only measure the first two damage mechanisms. Both indicators were proposed by Fehlemann et al. in [5]. The martensite cleavage fracture is quantified by counting the number of elements where the stress exceeds a previously set principal stress threshold, as these elements are expected to break. In the following, this indicator will be referred to as *cleavage fracture indicator.* In accordance to the work by Steinbrunner et al. this threshold is the stress at 5% of the martensite flow curve [18]. For estimating the martensite-ferrite grain-boundary decohesion, an indicator was proposed in [5], which determines the damage quantity by fitting a gumbel distribution to the stress values at the grain boundaries. The damage indicator is defined as the combination of the parameters describing the gumbel distribution. In this paper, this indicator will be referred to as *phase boundary decohesion (PBD) indicator*.

By analyzing the investigated points, the acquisition function chooses new interesting points in the design space that are used for the sRVE creation in the next epoch. The function aims to minimize both damage indicators simultaneously, finding Pareto-optimal states. The optimization is realized using the Python framework BoTorch which is meant for efficient Monte-Carlo based Bayesian optimization [19]. For this work, the *q-log noisy expected improvement* acquisition function was chosen since it is well suited for noisy data and is efficient for large batch sizes.

Results

The optimization was carried out over eleven epochs with 20 data points per epoch. As initial data, 50 data points were created. Since two sRVE are generated per microstructure configuration to reduce the influence of the scattering, 540 sRVE were created overall.

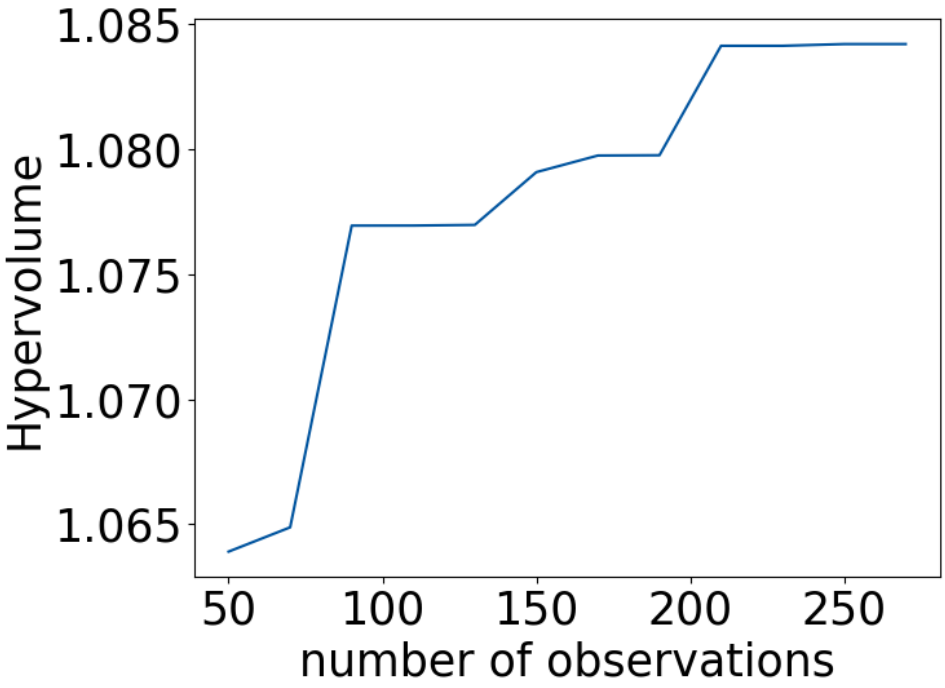

Fig 2. Evolution of the hypervolume of the Pareto front

Figure 2 shows the evolution of the hypervolume of the Pareto-front. The Pareto front is the set of all solutions in a multi-objective optimization problem for which no objective can be improved without worsening at least one other objective. The hypervolume is the size of the region in objective space that is dominated by the current nondominated set, and bounded by the reference point. The reference point is a user-chosen point in objective space, worse than all solutions of interest, used as the bounding corner for computing hypervolume. The choice of reference point influences the absolute value of the hypervolume, which is why only the trend can be interpreted. A larger hypervolume means, that the points are, on average, closer to the ideal, they cover more of the trade-off curve, not just one corner or that the spread of the Pareto front is better. I the hypervolume rises, the algorithm has found at least one new nondominated solution that expands the dominated region. Typically, the curve shows big jumps early into the optimization and smaller gains later. This is due to the algorithm quickly finding rough good regions and then fine-tuning the result.

The curve in the figure shows big jumps at the beginning, especially around 70 observations. Around 100 to 200 observations it stagnates, however it shows further jumps at 200 to 250 observations. The curve shows a monotone growth, meaning that every epoch offers an improvement of the knowledge of the Pareto-front. After 220 observations, no further improvements are made and the curve converges.

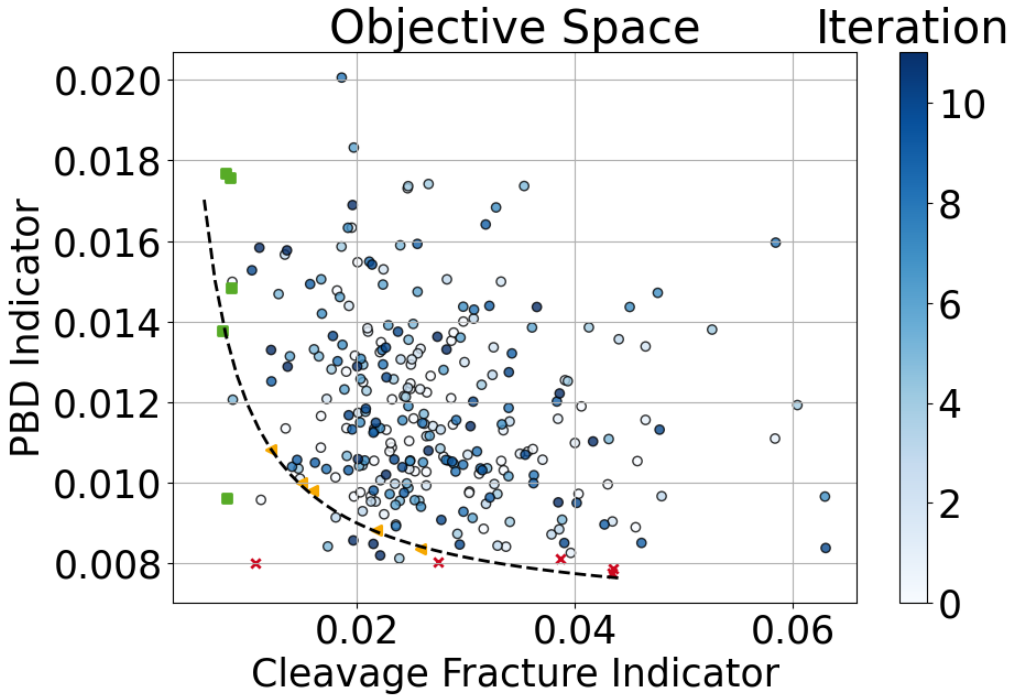

Fig 3. Scatter-Plot of the samples created in every optimization iteration, black dashed line: estimated Pareto-front, green rectangles: samples with the lowest cleavage fracture indicator, red crosses: samples with lowest phase boundary decohesion (PBD) indicator, yellow triangles: samples closest to estimated Pareto-front

Figure 3 shows the damage values achieved for all 270 microstructure combinations generated in the optimization. The plotted points are the average results from the two sRVE calculated for each microstructure parameter combination. The black dashed line illustrates the estimated Pareto-front achieved by the optimization. In a noise-free problem, no results on the left side of the line would be achievable. However, since the sRVE generation and load simulation are highly noisy and exhibit substantial scatter, some of the results are scattered beyond the front. The mean standard deviation of the calculated points from the plotted mean value is 0.0018 for the cleavage fracture indicator and 0.002 for the phase boundary decohesion indicator. This effect also makes the front less visible, which is why an approximation of the front was plotted as a dashed black line. The five data points closest to the front are marked as yellow triangles. Their microstructure parameter combinations are shown in **Figure 4**. Additionally, the data points resulting in the lowest cleavage fracture and phase boundary decohesion are marked as green rectangles and red crosses respectively. In **Figure 5**, the microstructure combinations corresponding to these states, that are optimal for one of the indicators are shown. The other datapoints are colored blue, with the shade according to the iteration they were generated in, as indicated by the color bar on the right side of the figure.

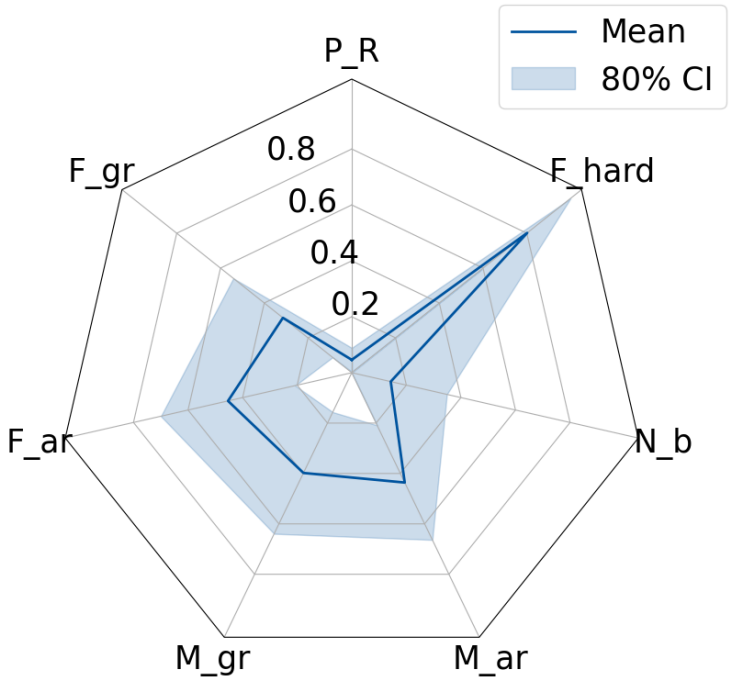

Fig 4. Mean microstructure parameter values of the samples closest to the Pareto front (orange triangles in Figure 2)

In **Figure 4**, the parameter values create in the last optimization epoch are shown in a radar chart. To make reading the image easier, all values are normalized to be between zero and one. A min-max normalization was used. The solid line depicts the mean value, while the shaded area is the 80% confidence interval (CI). If the confidence interval is large, this means, that there was a lot of variance in the parameters and vice-versa. A low variance implies, that the parameters' impact is high. The narrowest confidence interval is achieved for the phase ratio parameter.

For all data points, the values of this parameter remain very small. This means, that at the Pareto-front the sRVE contain large amounts of ferrite and only little martensite. The ferrite hardening parameter tends to be on the upper side of the parameter interval. This parameter also has a rather narrow confidence interval. The average of the band parameter is below 0.2, which means that in only one of the five sRVE a band was placed, while the other four sRVE did not contain a band. The grain size and aspect ratio parameters all have an average of about 0.4 with a wide confidence interval. Thus, most of the sRVE at the Pareto front have in common, that they have a low martensite content, no martensite bands and hard ferrite.

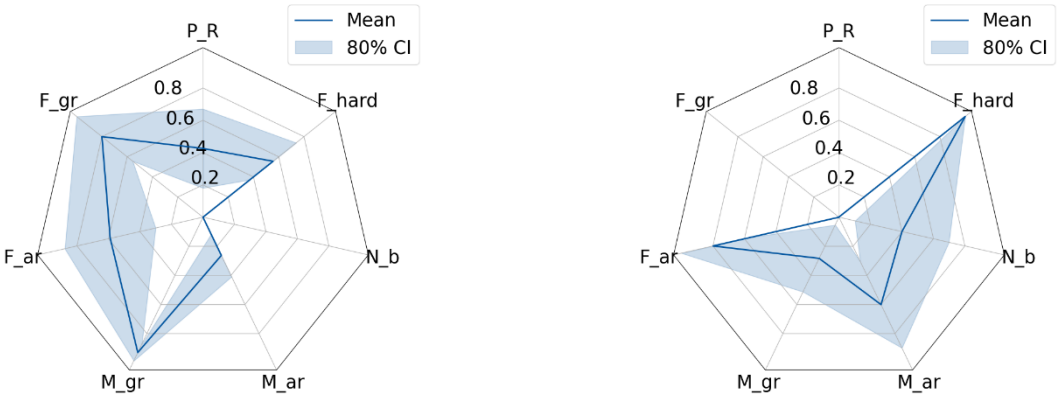

Fig 5. Radar Charts of the optimal microstructure configurations for minimal cleavage fracture (left) and phase boundary decohesion (right)

Figure 5 shows the mean microstructure configurations of the five sRVEs where the individual damage indicators are minimal. In **Figure 3** the shown sRVE are marked with red crosses (left side of this figure) and green rectangles (right side of this figure). Again, to make the comparison of the parameters easier, all values are normalized applying a min-max normalization to be between zero and one. By plotting the 80% confidence interval, the figure also shows the variance in each of the parameters.

The left side of the figure shows the results for the cleavage fracture indicator. The parameters with the smallest confidence interval are the number of bands, the martensite grain size and the aspect ratio of the martensite grains. The number of bands is zero with a confidence interval that is not visible, meaning that in the plotted data-set no bands were placed. The martensite aspect ratio is also below 0.4, while the martensite grain size is above 0.8. The narrow confidence interval implies, that these parameters are the most relevant ones when considering the martensite cleavage fracture. All of the ferrite parameters and the phase ratio have a wide confidence interval, which means, that the ferrite microstructure does not heavily influence martensite fracture.

On the right side of the figure the radar chart for the phase boundary decohesion indicator is depicted. The parameters with the lowest confidence intervals, and therefore the highest impact on the phase boundary decohesion, are the ferrite grain size and the phase ratio. Both lie at approximately zero. Another parameter with a narrow confidence interval is the ferrite hardening, where the mean value is at almost 1. The other parameters have a wide confidence interval, with a tendency for small martensite grains and a high ferrite aspect ratio.

Discussion

The results of the study show, which microstructure parameters promise minimal damage initiation during loading of DP steel. According to **Figure 4**, the most important microstructure feature to be controlled is the phase ratio of martensite and ferrite. It indicates, that microstructures with a low martensite content are more damage-resistant. Additionally, well distributed martensite that does not form bands is beneficial for the damage behavior of the material. Microstructures with a high ferrite hardening showed a better performance than those with softer ferrite.

These findings are mostly in line with the literature, which claims, that martensite cracking is facilitated by banding. Thus, material without martensite bands is generally more damage resistant. According to Asik [20], a higher martensite content also results in more damage initiation. This confirms in particular the results shown in the right side of **Figure 5**, where the optimal martensite content was shown to be the least possible. Additionally, Tasan et al. reports, that DP steel with larger martensite grains shows less phase boundary decohesion [3]. This can be explained by the larger area of the phase boundaries if the martensite grains are small, thus offering more sites for phase boundary decohesion. The same argument can be applied to the aspect ratio of the martensite, where a higher aspect ratio means, that the phase boundary area is larger. However, the right side of **Figure 5** shows the opposite. Here, the least phase boundary decohesion is achieved with small martensite grains with a low influence of the martensite aspect ratio. This can be explained by the way in which the used damage indicator works. It does not measure the absolute amount of decohesion sites but instead offers a statistical metric for the stress states at the phase boundaries. Thus, the indicator is not directly influenced by the area of the boundaries. This also explains the low impact of the martensite grain aspect ratio and the martensite bands on the phase boundary decohesion implied by the right side of the figure. Tian et al. claims, that a higher mechanical heterogeneity between ferrite and martensite causes a higher rate of phase boundary decohesion [8]. This matches the findings of this paper, which shows, that a higher ferrite hardening results in less damage initiation, especially for the grain boundary decohesion. Since the ferrite grain size also influences the phases mechanical properties, this also explains why a smaller grain size of the ferrite results in less damage initiation in the material. This is in line with the findings of Calcagnotto et al. [21] and the right side of **Figure 5**.

Figure 5 also illustrates why the underlying optimization task is rather complex. For all parameters, with the exception of the ferrite grain aspect ratio, the optimal states for the two damage indicators are essentially inverse to each other. In other words, parameter combinations that minimize

one damage indicator tend to be unfavorable with respect to the other. This antagonistic behavior indicates a pronounced trade-off between the two objectives: improving the performance of one damage indicator generally leads to a deterioration of the other.

In addition to these conflicting objectives, the problem is further complicated by substantial scatter in the simulation outcomes, as illustrated in **Figure 3**. The scatter is likely heteroscedastic in nature, meaning that the variance of the responses is not constant but varies across the design space. In some regions, the results are comparatively well clustered, while in others they exhibit a much larger spread. This heterogeneous variance structure reduces the robustness of local trends and makes it more challenging to reliably identify globally optimal parameter combinations. Overall, the combination of conflicting objectives and heteroscedastic scattering significantly increases the difficulty of the optimization task. This could be improved in future works by creating and averaging more than two RVE per parameter combination, so the scatter is minimized and the resulting damage values are as realistic as possible. However, this would make the simulations more computationally expensive which is why in this paper the number of RVEs per parameter combination was limited to two.

In the paper by Fehlemann et al., the Sobol indices for the considered microstructure parameters are calculated, which quantify the variance in the damage initiation caused by the parameters [5]. A high Sobol index implies a high impact of the parameter on the result. It is expected, that the parameters with high Sobol indices align with the ones showing a small confidence interval in **Figure 5.** In the paper, the martensite grain aspect ratio had the highest Sobol index for the cleavage fractur indicator. All of the other parameters' influence is calculated to be negligible. A similar result was observed by the confidence interval in this paper. However, according to this paper, the bands and the aspect ratio of martensite both have a big effect on the martensite fracture. The effects of bands and a high martensite aspect ratio can be attributed to the same mechanism, which can explain the discrepancy between the results of this paper and the one by Fehlemann et al. For the phase boundary decohesion, the cited paper predicts a high influence of the ferrite and martensite grain sizes, the phase ratio and the martensite aspect ratio. Out of these parameters, the only one with a wide confidence interval in **Figure 5** is the martensite aspect ratio. For the other parameters, the current paper backs the findings of Fehlemann et al.

In future works, the load case could be adapted to represent the actual stress states that appear during metal forming. This could be used to tailor damage resistant materials based on the processing route. Furthermore, the effect of using different damage indicators has to be analyzed. The indicator for martensite fracture should take into account, that the fracture is either ductile or semi-brittle after plastic deformation, as shown by recent research [22] [23] [24]. While cohesive zone modelling is probably more accurate for the prediction of the phase boundary decohesion, the implementation and calibration of such models is quite complicated. The indicator used in this paper offers a good tradeoff between the computational cost and the accuracy. In a future work, the phase boundary decohesion parameter could be further adapted to show the absolute amount of damage.

Furthermore, the performance of the optimization could be improved by reducing the number of considered parameters. For example, the martensite band parameter could be kept at zero, since the results of this study show, that damage resistant microstructures do not have bands. Additionally, parameters that were shown to have a low Sobol index for both of the damage indicators could also be removed from the optimization, since they are not expected to heavily influence the result.

Summary

This work presents the results of a multi-objective optimization study aimed at minimizing damage initiation during loading of DP800 dual-phase steel. In addition to identifying microstructure and parameter combinations that are most favorable for reducing overall damage, the study also determines those combinations that specifically minimize the initiation of individual damage mechanisms. The analysis includes a systematic evaluation of the influence and relative significance of the considered parameters on the optimization outcomes. It is shown that the optimization results are largely consistent with the literature, thereby supporting the validity of the approach and providing further insight into microstructure-property relationships in DP800 steel.

Acknowledgements

This research was funded by Deutsche Forschungsgemeinschaft (DFG, German Research Foundation; Projectnumber 278868966 – TRR 188; Damage Controlled Forming Processes, subproject B05).

References

[1] C. Tasan, M. Diehl, D. Yan, M. Bechthold, F. Roters, L. Schemman, C. Zheng, N. Periano, D. Ponge, M. Koyama, K. Tsuzaki, D. Raabe, An Overview of Dual-Phase Steels: Advances in Microstructure-Oriented Processing and Micromechanically Guided Design, Strength of materials 45 (2015) 391-431.

[2] A. Tekkaya, N. Khalifa, O. Hering, M. Rickmer, S. Myslicki, F. Walther, Forming-induced damage and its effects on product properties, CIRP Annals 66 (2017) 281-284.

[3] C. Tasan, J. Hoefnagels, D. Yan, F. Roters, D. Raabe, Strain localization and damage in dual phase steels investigated by coupled in-situ deformation experiments and crystal plasticity simulations, International Journal of Plasticity 63 (2014) 198-210.

[4] J. Mockus, Bayesian Approach to Global Optimization-Theory and Applications, first ed., Springer Dordrecht, 1989.

[5] N. C. Fehlemann, I. Biermann, S. Münstermann, Exploring structure–property relations in dual phase steels using crystal plasticity and variance based global sensitivity analysis, Materials & Design 259 (2025).

[6] F. Pütz, F. Shen, M. Könemann, S. Münstermann, The differences of damage initiation and accumulation of dp steels: a numerical and experimental analysis, International Journal Fracture 226 (2020) 1-15.

[7] N. C. Fehlemann, A. Medina, S. Lee, C. Kirchlechner, S. Münstermann, Crystal plasticity parameter identification via statistical relevant micropillar compression, Acta Materialia 297 (2025)

[8] C. Tian, C. Kusche, A. Medina, S. Lee, M. Wollenweber, R. Pippan, S. Korte-Kerzel, C. Kirchlechner, Understanding the damage initiation and growth mechanisms of two DP800 dual phase grades, Materials & Design 238 (2024).

[9] M. Henrich, N. Fehlemann, F. Bexter, M. Neite, L. Kong, F. Shen, M. Könemann, M. Dölz, S. Münstermann, DRAGen – A deep learning supported RVE generator framework for complex microstructure models, Heliyon 9 (2023).

[10] F. Roters, M. Diehl und P. Shanthraj, DAMASK -- The Düsseldorf Advanced Material Simulation Kit for Modelling Multi-Physics Crystal Plasticity, Damage, and Thermal Phenomena from the Single Crystal up to the Component Scale, Computational Materials Science 158 (2019), 420-478.

[11] I. Sobol, Uniformly distributed sequences with an additional uniform property, USSR Computational Mathematics and Mathematical Physics 16 (1976) 236-242.

[12] J. Rice, Inelastic constitutive relations for solids: An internalvariable theory and its application to metal plasticity, Journal of the Mechanics and Physics of Solids 19 (1971) 433–455.

[13] J. Hutchinson, Bounds and self-consistent estimates for creep of polycrystalline materials, Proceedings of the Royal Society of London A. Mathematical and Physical Sciences 348 (1976), 101-127.

[14] C. Tian, D. Ponge, L. Christiansen, C. Kirchlechner, On the mechanical heterogeneity in dual phase steel grades: Activation of slip systems and deformation of martensite in dp800, Acta Materialia 183 (2020) 274–284.

[15] J. Hodge, M. Orehoski, Relationship between hardenability and percentage of martensite in some low-alloy steels, Transactions of the American Institute of Mining and Metallurgical Engineers (1946), 627–642.

[16] L. Toth, The possibilities of the retained austenite reduction on tool steels, European Journal of Materials Science and Engineering 6 (2021).

[17] E. Pavlina, C. van Tyne, Correlation of yield strength and tensile strength with hardness for steels, Journal of Materials Engineering and Performance (2008) 888–893.

[18] D. Steinbrunner, D. Matlock, G. Krauss, Void formation during tensile testing of dual phase steels, Metallurgical transactions (1988), 579-589.

[19] M. a. K. B. Balandat, D. R. Jiang, S. Daulton, B. Letham, A. G. Wilson, E. Bakshy, BoTorch: A Framework for Efficient Monte-Carlo Bayesian Optimization, Advances in Neural Information Processing Systems 33 (2020).

[20] E. E. Asik, Damage in dual phase steels, University of Twente (2019).

[21] M. Calcagnotto, Y. Adachi, D. Ponge, D. Raabe, Deformation and fracture mechanisms in fine- and ultrafine-grained ferrite/martensite dual-phase steels and the effect of aging, Acta Materialia 59 (2011) 658-670.

[22] Y. Liang, S. Long, P. Xu, Y. Lu, Y. Jiang, Y. Liang, M. Yang, The important role of martensite laths to fracture toughness for the ductile fracture controlled by the strain in EA4T axle steel, Material Science and Engineering 695 (2017).

[23] S. Li, G. Zhu, Y. Kang, Effect of substructure on mechanical properties and fracture behavior of lath martensite in 0.1c–1.1si–1.7mn steel, Journal of Alloys and Compounds 675 (2016).

[24] F. Shen, S. Münstermann, J. Lian, A unified fracture criterion considering stress state dependent transition of failure mechanisms in bcc steels at –196 ∘C, International Journal of Plasticity 156 (2022).

[25] N. Fehlemann, A. Suarez Aguilera, S. Sandfeld, F. Bexter, M. Neite, D. Lenz, M. Könemann, S. Münstermann, Identification of martensite bands in dual–phase steels: a deep learning object detection approach using faster region–based–convolutional neural network, Steel Research International 94 (2023).

[26] N. Fehlemann, D. Czempas, M. Könemann, D. Lenz, G. Hirt, S. Münstermann, Investigation of Damage-Controlling Process-Parameters During Cold Rolling on the Impact Toughness of DP800 Steel Under Crash Loading Stress States, Proceedings of the 14th International Conference on the Technology of Plasticity - Current Trends in the Technology of Plasticity (2023).

[27] D. Peirce, R. Asaro, A. Needleman, Material rate dependence and localized deformation in crystalline solids, Acta Metallurgica (1983)1951–1976.

[28] D. Peirce, R. Asaro, A. Needleman, „An analysis of nonuniform and localized deformation in ductile single crystals,“ Acta Metallurgica 30 (1982) 1087–1119.

The publication of this article was funded by the RWTH Aachen University 10.13039/501100007210